

## Exotic Properties of $N^*(1895)$ and Its Impact on Photoproduction of Light Hyperons

K.P. KHEMCHANDANI<sup>a,\*</sup>, A. MARTÍNEZ TORRES<sup>b</sup>,  
SANG-HO KIM<sup>c</sup>, SEUNG-IL NAM<sup>c,d</sup> AND A. HOSAKA<sup>e,f</sup>

<sup>a</sup>Universidade Federal de São Paulo, C.P. 01302-907, São Paulo, Brazil

<sup>b</sup>Universidade de Sao Paulo, Instituto de Fisica, C.P. 05389-970, Sao Paulo, Brazil

<sup>c</sup>Department of Physics, Pukyong National University (PKNU), Busan 48513, Korea

<sup>d</sup>Asia Pacific Center for Theoretical Physics (APCTP), Pohang 37673, Korea

<sup>e</sup>Research Center for Nuclear Physics (RCNP), Osaka University, Ibaraki, Osaka, 567-0047, Japan

<sup>f</sup>Advanced Science Research Center, Japan Atomic Energy Agency (JAEA), Tokai 319-1195, Japan

Doi: [10.12693/APhysPolA.142.329](https://doi.org/10.12693/APhysPolA.142.329)

\*e-mail: [kanchan.khemchandani@unifesp.br](mailto:kanchan.khemchandani@unifesp.br)

In this work, we outline the findings of our recent study of the properties of  $N^*(1895)$  and its consequential impacts on the cross-sections of the photoproduction of  $\Lambda(1405)$ . Further, we discuss the possibility of the existence of an isovector state with a mass similar to  $\Lambda(1405)$ , which we refer to as  $\Sigma(1400)$ . With the idea of motivating experimental investigations of  $\Sigma(1400)$ , we have studied its photoproduction process and determined the respective cross-sections and polarization observables. We have studied also the coupling of  $N^*(1895)$  to  $K\Sigma(1400)$  and found that it gives an important contribution to the cross-sections near the threshold. In the process, we have determined the branching ratios of the decay of  $N^*(1895)$  to the final states involving  $\Lambda(1405)$  and  $\Sigma(1400)$  to be in the range of 6–7 MeV. Our findings can motivate the consideration of alternative processes in partial wave analyses of experimental data when studying the properties of  $N^*(1895)$ .

topics: properties of unstable baryons, effective Lagrangian approach

### 1. Introduction

The nature of interactions in meson–baryon systems with strangeness  $-1$  leads to several interesting questions, like the existence of exotic nuclear matter, the kaonic nuclei, the possibility of the presence of strange matter in neutron stars, etc. (see [1–3] for recent discussions on the topic). The key to finding an answer to these questions is understanding the nature of hyperons, especially  $\Lambda(1405)$ . Indeed, there exists an extensive discussion on the nature of  $\Lambda(1405)$ , attributing its origin to the meson–baryon dynamics (some of the most cited works on the topic are [4–13]). The state is, hence, referred to as a dynamically generated hyperon or a molecular hyperon. Such a description is what raises the question of binding more and more nucleons to kaons (through coupled channel interactions). Furthermore, there are persistent discussions on associating two complex energy poles to  $\Lambda(1405)$ , one coupling strongly to  $\bar{K}N$  and the other to  $\pi\Sigma$  (for the latest review, see [14]). Most theoretical investigations agree on the position of one of the poles, which lies closer to the real axis and to the  $\bar{K}N$  thresh-

old. However, different works differ on the position of the pole lying deeper in the complex plane. It is also important to acknowledge the growing efforts made by the experimental [15–17] and lattice groups [18–24], clearly showing the importance of the topic. It is important to mention before continuing the discussions that although our focus is on strangeness  $-1$  here, the existence of exotic nuclear matter without strangeness is also a hot topic of research [25, 26].

Though  $\Lambda(1405)$  gets the dominant focus in the strangeness  $-1$  sector, some works indicate the possibility of the presence of a similar, but isovector, hyperon [12, 27–33] in the experimental data. The situation is far from clear and more studies are required to reach any conclusions. Our study of meson–baryon interactions with strangeness  $-1$  in [34] showed that the existing experimental data indicate the presence of such an isovector state. We refer to it as  $\Sigma(1400)$ . The experimental data considered in [34] were total cross-sections on different processes with  $K^-p$  initial state, energy level shift, and width of the  $1s$  state of the kaonic hydrogen, and the ratios of cross-sections of the different processes near the  $K^-p$  threshold.

To motivate experimental studies of  $\Sigma(1400)$ , we determine different observables for its photoproduction [35]. At the same time, we study the photoproduction of  $\Lambda(1405)$ , on which experimental data is already available. In this way, we test our model by comparing our results with the experimental data. Also, we calculate polarization observables for both hyperons, on which data is not available. Our results can be useful for future experimental studies, including those on  $\Lambda(1405)$ . In fact, better statistics data on  $\Lambda(1405)$  production is expected to come in the future from the ELSA facility [36].

The model of photoproduction of the light hyperons, considered in our work, is based on different  $s$ -,  $t$ -, and  $u$ -channel diagrams, including the exchange of relevant hyperon/nucleon resonances using effective Lagrangians. The couplings at the different vertices are determined from the coupled channel meson–baryon amplitudes, which generate the light hyperon resonances. To extend the applicability of the model beyond the threshold region, we use the Regge approach. We also consider the exchange of different nucleon resonances with mass close to the  $KH^*(1400)$  threshold, where  $H^*(1400)$  stands for  $\Lambda(1405)$  and  $\Sigma(1400)$ . We find that the most important contribution comes from  $N^*(1895)$ , which was found to have large meson–baryon coupling in [37]. In the mentioned work, two poles with overlapping widths were found to arise in the complex plane, which interfered and produced a single peak on the real axis around 1900 MeV. The decay properties of  $N^*(1895)$  were investigated more recently, in [38], using its coupling to different meson–baryon channels obtained in the earlier work [37]. The study showed that the decay width of  $N^*(1895)$  to  $KH^*$  is considerable, thus, offering alternative processes to study the properties of the nucleon resonance.

## 2. Formalism and results

Let us begin the discussions by briefly mentioning the Lagrangians considered in our works to study meson–baryon scattering. For the vector meson–baryon interactions, we write [39]

$$\begin{aligned} \mathcal{L}_{VB} = & -g \left\{ \langle \bar{B} \gamma_\mu [V_8^\mu, B] \rangle + \langle \bar{B} \gamma_\mu B \rangle \langle V_8^\mu \rangle \right. \\ & + \frac{1}{4M} \left( F \langle \bar{B} \sigma_{\mu\nu} [V_8^{\mu\nu}, B] \rangle + D \langle \bar{B} \sigma_{\mu\nu} \{V_8^{\mu\nu}, B\} \rangle \right) \\ & \left. + \langle \bar{B} \gamma_\mu B \rangle \langle V_0^\mu \rangle + \frac{C_0}{4M} \langle \bar{B} \sigma_{\mu\nu} V_0^{\mu\nu} B \rangle \right\}, \end{aligned} \quad (1)$$

where the subscript 8 (0) denotes the octet (singlet) part of the wave function of the vector meson (relevant in the case of  $\omega$  and  $\phi$ ),  $V^{\mu\nu}$  represents the tensor field of the vector mesons,

$$V^{\mu\nu} = \partial^\mu V^\nu - \partial^\nu V^\mu + ig [V^\mu, V^\nu], \quad (2)$$

and

$$g = \frac{m_v}{\sqrt{2} f_v}, \quad (3)$$

with  $m_v$  ( $f_v$ ) being the mass (decay constant) of a given vector meson in the vertex and the constants  $D = 2.4$ ,  $F = 0.8$ , and  $C_0 = 3F - D$ .

TABLE I

The poles related to  $N^*(1895)$ ,  $\Lambda(1405)$  and  $\Sigma(1400)$  as obtained in [34, 37].

State	Pole position		Ref.
	$E - i\Gamma/2$ [MeV]		
$N^*(1895)$	1801 – i96	1912 – i54	[37]
$\Lambda(1405)$	1385 – i124	1426 – i15	[34]
$\Sigma(1400)$	1399 – i36		[34]

To determine the amplitudes for the systems consisting of pseudoscalar mesons and baryons, we use the lowest order chiral Lagrangian [10–12, 40–43]

$$\begin{aligned} \mathcal{L}_{PB} = & \langle \bar{B} i \gamma^\mu \partial_\mu B + \bar{B} i \gamma^\mu [\Gamma_\mu, B] \rangle - M_B \langle \bar{B} B \rangle \\ & + \frac{1}{2} D' \langle \bar{B} \gamma^\mu \gamma_5 \{u_\mu, B\} \rangle + \frac{1}{2} F' \langle \bar{B} \gamma^\mu \gamma_5 [u_\mu, B] \rangle, \end{aligned} \quad (4)$$

where  $u_\mu = i u^\dagger \partial_\mu U u^\dagger$ , and

$$\Gamma_\mu = \frac{1}{2} (u^\dagger \partial_\mu u + u \partial_\mu u^\dagger), \quad (5)$$

$$U = u^2 = \exp(iP/f_P), \quad (6)$$

with  $f_P$  representing the pseudoscalar decay constant,  $P$  ( $B$ ) denoting the matrices of the octet meson (baryon) fields, and  $F' = 0.46$  and  $D' = 0.8$ .

The transition amplitudes between the pseudoscalar–baryon and the vector–baryon channels are deduced through [44]

$$\begin{aligned} \mathcal{L}_{PBVB} = & -\frac{i g_{PBVB}}{2 f_v} \left( F' \langle \bar{B} \gamma_\mu \gamma_5 [[P, V^\mu], B] \rangle \right. \\ & \left. + D' \langle \bar{B} \gamma_\mu \gamma_5 \{[P, V^\mu], B\} \rangle \right). \end{aligned} \quad (7)$$

Using the aforementioned Lagrangians we determine the amplitudes for different meson–baryon systems, for different  $s$ -,  $t$ -,  $u$ -channels and contact interactions (see [34, 37, 39] for more details). We solve Bethe–Salpeter equation with these amplitudes and look for poles in the complex plane, which are identified with baryon resonances. Within such a formalism, dynamical generation of  $N^*(1895)$ ,  $\Lambda(1405)$  and  $\Sigma(1400)$  was found in the strangeness 0 [37] and  $-1$  systems [34]. The complex energy poles related to these states, as found in [34, 37], are given in Table I.

As can be seen in Table I, two poles are related to both  $N^*(1895)$  as well as  $\Lambda(1405)$ . The strangeness  $-1$  amplitudes were constrained to fit the data on the energy level shift and width of the  $1s$  state of the kaonic hydrogen [45] and cross-section data (summarized in [46]) on the processes:  $K^- p \rightarrow K^- p$ ,  $\bar{K}^0 n$ ,  $\eta \Lambda$ ,  $\pi^0 \Lambda$ ,  $\pi^0 \Sigma^0$ ,  $\pi^\pm \Sigma^\mp$ . In the case of non-strange systems, the amplitudes reproduced well the isospin  $1/2$  and  $3/2$   $\pi N$  amplitudes extracted from partial wave analysis [47] and the  $\pi^- p \rightarrow \eta n$  and  $\pi^- p \rightarrow K^0 \Lambda$  cross-sections up to a total energy of about 2 GeV.

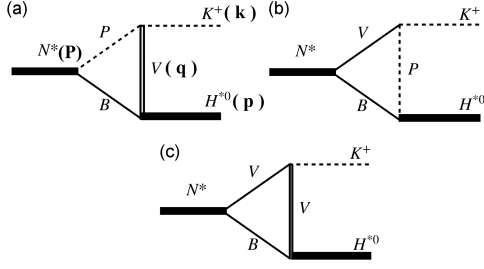


Fig. 1. Different diagrams contributing to the decay of  $N^*(1895)$  to  $K\Lambda(1405)$  and  $K\Sigma(1400)$ .

Before proceeding further, a few words on the known information related to  $N^*(1895)$ . This  $S_{11}$  nucleon resonance appears after  $N^*(1535)$  and  $N^*(1620)$  and has been listed as  $N^*(2090)$  ( $J^\pi = 1/2^-$ ) in the compilations earlier than 2012 of the particle data group (PDG). All  $1/2^-$  states found in partial wave analyses of relevant experimental data are catalogued together under the label of  $N^*(1895)$ , hence their properties are associated with large uncertainties. Indeed, nucleon resonances around 1890 MeV are not well understood since most of the information in this energy region is extracted from the data on reactions producing  $K\Lambda$  and  $K\Sigma$  final states and different  $N^*$ 's couple with similar strength to these channels. For example, different descriptions have been brought forward for the peak present around 1900 MeV in the  $\gamma p \rightarrow K^+\Lambda$  total cross-sections [48–52]. Furthermore, different quark models [53–56] predict a different mass for the third  $S_{11}$  state, with the values lying near 2 GeV.

In such a scenario, detailed studies of the properties of  $N^*(1895)$  are very much required. Keeping this in mind, and using the fact that  $N^*(1895)$  was found to strongly couple to meson–baryon systems in [37], we made further investigations of its decay properties in [38]. Using the couplings to different meson–baryon channels obtained in the previous work [37], we investigated the decay processes of  $N^*(1895)$  to final states with  $H^*(1400)$  through the diagrams shown in Fig. 1.

The vertices involving the nucleon/hyperon resonances are written in [38] as

$$\begin{aligned}\mathcal{L}_{N^*PB} &= ig_{PB N^*} \bar{B} N^* P^\dagger, \\ \mathcal{L}_{N^*VB} &= -\frac{i}{\sqrt{3}} g_{VB N^*} \bar{B} \gamma_5 \gamma_\mu N^* V^{\mu\dagger}, \\ \mathcal{L}_{PBH^*} &= g_{PBH^*} P \bar{H}^* B, \\ \mathcal{L}_{VBH^*} &= \frac{i}{\sqrt{3}} g_{VBH^*} V^\mu \bar{H}^* \gamma_\mu \gamma_5 B,\end{aligned}\quad (8)$$

and the remaining ones as

$$\mathcal{L}_{PPV} = -ig_{PPV} \langle V^\mu [P, \partial_\mu P] \rangle, \quad (9)$$

$$\mathcal{L}_{VVP} = \frac{1}{\sqrt{2}} g_{VVP} \epsilon^{\mu\nu\alpha\beta} \langle \partial_\mu V^\nu \partial_\alpha V_\beta P \rangle. \quad (10)$$

In (8) the field  $H^*$  represents  $\Sigma(1400)$  or  $\Lambda(1405)$ , and the factor  $\sqrt{3}$  in the Lagrangians,  $\mathcal{L}_{N^*VB}$  and  $\mathcal{L}_{VBH^*}$ , appears due to the fact that the spin-projected amplitudes were parameterized as Breit–Wigner in [34, 37] when calculating the meson–baryon resonance couplings.

The formalism lead to finding of amplitudes as

$$\begin{aligned}t_a &= i \sum_j g_{VBH^*,j} g_{PB N^*,j} g_{PPV} C_j \bar{u}_{H^*}(p) \gamma_\nu \gamma_5 \\ &\times \int \frac{d^4q}{(2\pi)^4} \left[ \frac{\not{P} - \not{k} + \not{q} + m_{Bj}}{(P-k+q)^2 - m_{Bj}^2 + i\epsilon} \right. \\ &\times \left. \frac{\left( -g^{\nu\mu} + \frac{q^\nu q^\mu}{m_{Vj}^2} \right)}{q^2 - m_{Vj}^2 + i\epsilon} \frac{(2k-q)_\mu}{(k-q)^2 - m_{Pj}^2 + i\epsilon} \right] u_{N^*}(P),\end{aligned}\quad (11)$$

where the momenta associated to the different hadrons are as shown in Fig. 1a. The labels  $P$ ,  $V$ , and  $B$  in Fig. 1 refer to all the different possible pseudoscalar, vector meson, and baryon channels, which can contribute to the loop. All such contributions are summed through the index  $j$  in (11). The constant  $C_j$  in (11) is a coefficient coming from the trace in (9) for the VPP vertex, and  $m_{Bj}$ ,  $m_{Vj}$ , and  $m_{Pj}$  are the masses of the baryon, vector, and pseudoscalar meson, respectively, corresponding to the  $j$ -th channel in the triangular loop. The values of the different  $C_j$  coefficients are given in [38].

The product of the spinors, gamma matrices, and the numerator of the expression within the curly brackets in (11) gives the expression

$$\begin{aligned}N_a(q) &= (4kp - 2pq - q^2) \bar{u}_{H^*}(p) \gamma_5 u_{N^*}(P) \\ &- 2(M_{H^*} + m_{Bj}) \bar{u}_{H^*}(p) \not{k} \gamma_5 u_{N^*}(P) \\ &\times (M_{H^*} + m_{Bj}) \bar{u}_{H^*}(p) \not{q} \gamma_5 u_{N^*}(P) \\ &+ 2 \bar{u}_{H^*}(p) \not{k} \not{q} \gamma_5 u_{N^*}(P) \\ &+ \frac{(2kq - q^2)}{m_{Vj}^2} \left[ (M_{H^*} + m_{Bj}) \bar{u}_{H^*}(p) \not{q} \gamma_5 u_{N^*}(P) \right. \\ &\left. - (2pq + q^2) \bar{u}_{H^*}(p) \gamma_5 u_{N^*}(P) \right],\end{aligned}\quad (12)$$

where  $M_{H^*}$  is the mass of  $H^*(1400)$ . The integration on the zeroth component of the four momentum in (11) can be done analytically, using Cauchy's theorem. To do so, we reorganize (12) by writing it as a series of terms depending on different powers of  $q^0$ . In this way, the amplitude gets written as

$$\begin{aligned}t_a &= i \sum_j g_{VBH^*,j} g_{PB N^*,j} g_{PPV} \mathcal{N}_{H^*} \mathcal{N}_{N^*} C_j \\ &\int \frac{d^4q}{(2\pi)^4} \frac{\left\{ \chi^\dagger \left( \sum_{i=0}^4 \mathcal{A}_{i,j} [q^0]^i \right) \chi \right\}}{[(P-k+q)^2 - m_{Bj}^2 + i\epsilon]} \\ &\times \frac{1}{[q^2 - m_{Vj}^2 + i\epsilon]} \frac{1}{[(k-q)^2 - m_{Pj}^2 + i\epsilon]},\end{aligned}\quad (13)$$

where a typical coefficient of  $[q^0]^i$ , for  $i = 0$ , looks like

$$\begin{aligned} \mathcal{A}_{0,j} = (\boldsymbol{\sigma} \cdot \mathbf{k}) & \left[ 2(M_{H^*} + m_{B_j}) + \frac{1}{E_{H^*} + M_{H^*}} \right. \\ & \times \left( 2k^0(M_{H^*} + m_{B_j} + 2E_{H^*}) - 2\mathbf{k} \cdot \mathbf{q} + |\mathbf{q}|^2 \right. \\ & \left. \left. + 4|\mathbf{k}|^2 + \frac{|\mathbf{q}|^4 + 4(\mathbf{k} \cdot \mathbf{q})^2 - 4(\mathbf{k} \cdot \mathbf{q})|\mathbf{q}|^2}{m_{V_j}^2} \right) \right] \\ & - (\boldsymbol{\sigma} \cdot \mathbf{q}) \left[ (M_{H^*} + m_{B_j}) \left( 1 - \frac{2\mathbf{k} \cdot \mathbf{q} - |\mathbf{q}|^2}{m_{V_j}^2} \right) \right. \\ & \left. + 2k^0 + \frac{2|\mathbf{k}|^2}{E_{H^*} + M_{H^*}} \right]. \end{aligned} \quad (14)$$

The coefficients of other powers of  $q^0$  can be found in [38]. After integrating on  $q^0$ , we find the expression to be numerically integrated

$$\begin{aligned} t_a = i \sum_j g_{VBH^*,j} g_{PB N^*,j} g_{PPV} C_j \mathcal{N}_{H^*} \mathcal{N}_{N^*} \\ \times \int d\Omega_q \int_0^{\Lambda} \frac{d|\mathbf{q}| |\mathbf{q}|^2}{(2\pi)^3} \sum_{i=0}^4 \chi^\dagger \mathcal{A}_{i,j}(\mathbf{q}) \chi \frac{(-iN_{i,j}(\mathbf{q}))}{\mathcal{D}_j(\mathbf{q})} \end{aligned} \quad (15)$$

with

$$\begin{aligned} \frac{(-iN_{i,j}(\mathbf{q}))}{\mathcal{D}_j(\mathbf{q})} & \equiv \int \frac{dq^0}{(2\pi)} \frac{(q^0)^i}{[(P-k+q)^2 - m_{B_j}^2 + i\epsilon]} \\ & \times \frac{1}{[q^2 - m_{V_j}^2 + i\epsilon] [(k-q)^2 - m_{P_j}^2 + i\epsilon]}. \end{aligned} \quad (16)$$

Detailed analytical expressions for  $N_{i,j}$  and  $\mathcal{D}_j$  are given [38]. A cut-off  $\Lambda \simeq 600\text{--}700$  MeV is used in the integration on the three-momentum consistently with the work in [34, 37], where relevant experimental data were reproduced by different meson–baryon amplitudes.

Finally, the final states are projected on  $p$ -wave through

$$\begin{aligned} \langle t_a \rangle = i \sum_j g_{VBH^*,j} g_{PB N^*,j} g_{PPV} \mathcal{N}_{H^*} \mathcal{N}_{N^*} C_j \\ \times \left[ \frac{1}{2} \int_{-1}^1 d\cos(\theta) (-\cos(\theta)) \int d\Omega_q \int_0^{\Lambda} \frac{d|\mathbf{q}|}{(2\pi)^3} |\mathbf{q}|^2 \right. \\ \sum_{i=0}^4 \chi^\dagger \mathcal{A}_{i,j}(\mathbf{q}) \chi \frac{(-iN_{i,j}(\mathbf{q}))}{\mathcal{D}_j(\mathbf{q})} \\ \left. + \frac{1}{2} \int_{-1}^1 d\cos(\theta) (-\sin(\theta)) \int d\Omega_q \int_0^{\Lambda} \frac{d|\mathbf{q}|}{(2\pi)^3} |\mathbf{q}|^2 \right. \\ \left. \sum_{i=0}^4 \chi^\dagger \mathcal{A}_{i,j}(\mathbf{q}) \chi \frac{(-iN_{i,j}(\mathbf{q}))}{\mathcal{D}_j(\mathbf{q})} \right], \end{aligned} \quad (17)$$

where the directions of the arrows in the subscript indicate the spinors of  $H^*$  and  $N^*$ .

TABLE II

Branching ratios (in the isospin base) of the two poles of  $N^*(1895)$  to different final states.

Decay channel	Branching ratios [%]		Experimental data [57]
	$N_1^*(1895)$	$N_2^*(1895)$	
$\pi N$	9.4	10.8	2–18
$\eta N$	2.7	18.1	15–40
$K\Lambda$	10.9	19.4	13–23
$K\Sigma$	0.7	26.0	6–20
$\rho N$	5.6	3.5	< 18
$\omega N$	25.7	6.2	16–40
$\phi N$	8.9	1.1	–
$K^* \Lambda$	12.1	14.0	4–9
$K^* \Sigma$	6.1	0.3	–
$K\Lambda_1^*$	$5.4 \pm 0.7$	$1.8 \pm 0.1$	–
$K\Lambda_2^*$	$3.3 \pm 0.4$	$1.1 \pm 0.2$	–
$K\Sigma^*$	$5.9 \pm 0.8$	$11.2 \pm 1.1$	–

The amplitudes for other diagrams in Fig. 1 are obtained similarly, and explicit expressions can be found in [38]. The results obtained on the branching ratios are summarized in Table II, where the subscripts on  $\Lambda^*$  and  $N^*(1895)$  refer to the two poles related to each one of them.

It can be seen that the results obtained are in good agreement with the available data and that the branching ratios for decay to light hyperons are comparable to meson–baryon decay channels. It should be recalled at this point that no free parameters are involved in the determination of the partial decay widths. The couplings for each vertex have been taken from our former works [34, 37], where  $N^*(1895)$  and  $H^*(1400)$  have been found to arise from meson baryon dynamics. Such information can be helpful in using experimental data on  $\Lambda(1405)$  production to study the properties of  $N^*(1895)$ .

Our findings summarized in Table II imply that the exchange of  $N^*(1895)$  in the  $s$ -channel can play an important role in describing processes with a  $K\Lambda(1405)$  final state. In fact, we studied the photoproduction of  $\Lambda(1405)$  in [35], considering the diagrams shown in Fig. 2. As can be seen in Fig. 2, we consider the exchange of (several) nucleon resonances (those lying close to the  $KH^*(1400)$  threshold). To consider the exchange of  $N^*(1895)$ , we determined amplitudes for the  $N^*(1895) \rightarrow KH^*(1400)$  vertex, where the mass of  $N^*(1895)$  and  $H^*(1400)$  vary within the respective range allowed by the respective, associated, widths. Such amplitudes can be found in [38].

Further, we determined the radiative decays of  $N^*(1895)$  and  $H^*(1400)$ , to calculate the diagrams shown in Fig. 2. To do this, we consider the vector meson dominance mechanism and use the Lagrangian [58]

$$\mathcal{L}_{V\gamma} = -\frac{eF_V}{2} \lambda_{V\gamma} V_{\mu\nu} A^{\mu\nu}, \quad (18)$$

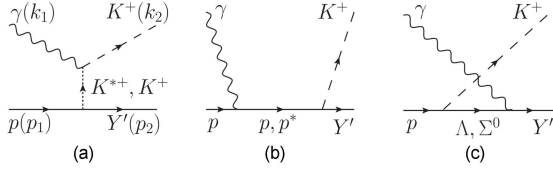


Fig. 2. Diagrams contributing to the photoproduction of  $\Lambda(1405)$  and  $\Sigma(1400)$  (denoted as  $Y'$  in the diagrams).

TABLE III

Radiative decay widths for  $\Lambda(1405)$ ,  $\Sigma(1400)$  and  $N^*(1895)$ . In all the results shown here, an interference between the two poles related to the decaying hadron has been considered to obtain the decay width.

Decay process	Partial width [KeV]
$\Lambda(1405) \rightarrow \Lambda\gamma$	$26.19 \pm 6.93$
$N^*(1895) \rightarrow p\gamma$	$650.70 \pm 65.10$
$\Sigma(1400) \rightarrow \Lambda\gamma$	$49.97 \pm 8.57$
$\Sigma(1400) \rightarrow \Sigma\gamma$	$94.51 \pm 9.33$
$\Lambda(1405) \rightarrow \Sigma\gamma$	$2.50 \pm 1.37$

where  $F_V$  is the decay constant for vector mesons,

$$A^{\mu\nu} = \partial^\mu A^\nu - \partial^\nu A^\mu, \quad (19)$$

$V_{\mu\nu}$  is a tensor field related to  $\rho^0$ ,  $\omega$ , and  $\phi$ , with  $\lambda_{V\gamma} = 1, \frac{1}{3}$ , and  $-\frac{\sqrt{2}}{3}$ , respectively, and

$$V^{\mu\nu} = \frac{1}{M_V} (\partial^\mu V^\nu - \partial^\nu V^\mu). \quad (20)$$

Consequently we obtain the amplitude for the  $B^* \rightarrow B\gamma$  process as

$$t_{B^* \rightarrow B\gamma} = \frac{2eF_V \tilde{g}_{VBB^*} \lambda_{V\gamma}}{M_V^2} \bar{B} \gamma_5 \not{\epsilon} \mathcal{K} B^*, \quad (21)$$

with  $\epsilon$  denoting the polarization vector for the photon, and plug it in the following equation to determine the width,

$$\Gamma_{B^* \rightarrow B\gamma} = \frac{|\mathcal{K}| (4M_{B^*} M_B)}{32\pi^2 M_{B^*}^2} \frac{1}{2S_{B^*} + 1} \times \int d\Omega \sum_{B^*, m_B, m_\gamma} |\mathcal{M}_{B^* \rightarrow B\gamma}|^2. \quad (22)$$

The results obtained on the radiative decay widths are given in Table III.

The radiative decay width of  $\Lambda(1405) \rightarrow \Lambda\gamma$ , listed by PDG, is  $27 \pm 8$  KeV [57]. It can be seen that our result is in remarkable agreement with the experimental data [57]. For  $\Lambda(1405) \rightarrow \Sigma\gamma$ , PDG [57] provides two possible values, namely  $10 \pm 4$  KeV or  $23 \pm 7$  KeV. Our results are closer to the former value. It is more complex to draw conclusions on the partial width obtained for the  $N^*(1895)$  radiative decay by comparing them with the information provided by PDG, since two complex energy poles associated with it will be required in partial wave analysis. Still, we can say that our results for the

second pole seem to be closer to the upper limit of the value, 0.01–0.06, given in [57]. The former finding is consistent with a better agreement between the real and imaginary part of the second pole of  $N^*(1895)$  found in our work and the values associated with  $N^*(1895)$  in [57].

We are now in a position to discuss the effective Lagrangians used in our model to calculate the photoproduction cross-sections. For the electromagnetic vertices, we write

$$\begin{aligned} \mathcal{L}_{\gamma KK} &= -ie \left[ K^\dagger (\partial_\mu K) - (\partial_\mu K^\dagger) K \right] A^\mu, \\ \mathcal{L}_{\gamma KK^*} &= g_{\gamma KK^*}^c \epsilon^{\mu\nu\alpha\beta} \partial_\mu A_\nu \\ &\quad \times \left[ (\partial_\alpha K_\beta^{*-}) K^+ + K^- (\partial_\alpha K_\beta^{*+}) \right], \\ \mathcal{L}_{\gamma NN} &= -\frac{e}{2} \bar{N} \left[ \gamma_\mu (1 + \tau_3) - \frac{1}{M_N} \kappa_N \sigma_{\mu\nu} \partial^\nu \right] A^\mu N, \\ \mathcal{L}_{\gamma YY^*} &= \frac{e}{2M_N} \mu_{Y^*Y} \bar{Y} \gamma_5 \sigma_{\mu\nu} \partial^\nu A^\mu Y^* + \text{h.c.}, \end{aligned} \quad (23)$$

where  $A^\mu$  is the photon field,  $Y$  denotes  $\Lambda(1116)$  or  $\Sigma^0(1192)$ , the coupling constant  $g_{\gamma KK^*}^c$  is determined from the experimental data for  $\Gamma_{K^{*+} \rightarrow K^+ \gamma}$  [57] to be  $0.254 \text{ GeV}^{-1}$ ,  $\kappa_p = 1.79$  [57] is the proton anomalous magnetic moment, and  $\mu_{Y^*Y}$  represents transition magnetic moments.

Further, effective Lagrangians required at the strong vertices are taken as

$$\begin{aligned} \mathcal{L}_{KNY} &= -ig_{KNY} \bar{N} \gamma_5 Y K + \text{h.c.}, \\ \mathcal{L}_{KNY^*} &= g_{KNY^*} \bar{K} \bar{Y}^* N + \text{h.c.}, \\ \mathcal{L}_{K^*NY^*} &= \frac{i}{\sqrt{3}} g_{K^*NY^*} \bar{K}^{*\mu} \bar{Y}^* \gamma_\mu \gamma_5 N + \text{h.c.}, \end{aligned} \quad (24)$$

where  $g_{KN(\Lambda, \Sigma^0)} = (-13.4, 4.09)$  [59, 60]. The values for the  $Y^* \bar{K} N$  and  $Y^* \bar{K}^* N$  couplings are taken from [34]. The factor  $\frac{1}{\sqrt{3}}$  in  $\mathcal{L}_{K^*NY^*}$  takes into account the fact that the Lagrangian has a spin structure, while the couplings in [34, 37] are obtained by evaluating the residue of the spin-projected  $t$ -matrices.

In order to extend the applicability of our model beyond the threshold region, we use a hybridized Regge model. This is done by replacing the Feynman propagators for  $K$  and  $K^*$  by the Regge expressions

$$\begin{aligned} \frac{1}{t - M_K^2} &\rightarrow (s/s_0^K)^{\alpha_K(t)} \left\{ \begin{array}{c} 1 \\ e^{-i\pi\alpha_K(t)} \end{array} \right\} \\ &\times \frac{\pi\alpha_{K'}}{\sin(\pi\alpha_K(t))} \frac{1}{\Gamma(1 + \alpha_K(t))}, \end{aligned} \quad (25)$$

and

$$\begin{aligned} \frac{1}{t - M_{K^*}^2} &\rightarrow (s/s_0^{K^*})^{\alpha_{K^*}(t)-1} \left\{ \begin{array}{c} 1 \\ e^{-i\pi\alpha_{K^*}(t)} \end{array} \right\} \\ &\times \frac{\pi\alpha'_{K^*}}{\sin(\pi\alpha_{K^*}(t))} \frac{1}{\Gamma(\alpha_{K^*}(t))}, \end{aligned} \quad (26)$$

where

$$\alpha_K(t) = 0.7 \text{ GeV}^{-2} (t - M_K^2), \quad (27)$$

$$\alpha_{K^*}(t) = 1 + 0.83 \text{ GeV}^{-2} (t - M_{K^*}^2),$$

with

$$\alpha'_{K,K^*} \equiv \frac{\partial \alpha_{K,K^*}(t)}{\partial t}, \quad (28)$$

and  $s_0^K = 3.0 \text{ GeV}^2$  and  $s_0^{K^*} = 1.5 \text{ GeV}^2$ . More details on the formalism can be found in [35].

In Fig. 3, we show our results on the photoproduction cross-sections for the case of  $\Lambda(1405)$  as a function of the beam energy. It can be seen that our results (shown as a continuous line) are in good agreement with the data obtained by the CLAS Collaboration [17]. The contributions to the full results from different sources are also shown in Fig. 3. The dotted curve shows the contribution from the kaon Reggeon plus the electric part of the nucleon exchange (the sum is a gauge invariant contribution). The dot-dashed and the dot-dashed-dashed curves show the  $K^*$ -Reggeon and the exchange of  $N^*$ 's, respectively. The dashed curve depicts the total contributions from the Born diagrams.

The nucleon resonances considered in the  $s$ -channel exchange are:  $N^*(1895)$ ,  $N^*(2000, 5/2^+)$ ,  $N^*(2100, 1/2^+)$ ,  $N^*(2030, 1/2^-)$ ,  $N^*(2055, 3/2^-)$ , and  $N^*(2095, 3/2^-)$ . However, the contributions from the states other than  $N^*(1895)$  are found to be small, and the exchange of  $N^*(1895)$  plays an important role in describing the data in the low-energy region ( $E_\gamma \leq 2.5 \text{ GeV}$ ).

We also predict the cross-sections for the process  $\gamma p \rightarrow K^+ \Sigma(1400)$ . The results are shown in Fig. 4. The order of magnitude of the cross-sections shown in Fig. 4 will be measurable in the future.

It should be pointed out that also in this case, the  $N^*(1895)$  exchange in the  $s$ -channel provides important contributions to the cross-sections near the threshold. It can be noticed that the cross-sections coming from the  $N^*$ -exchange give rise

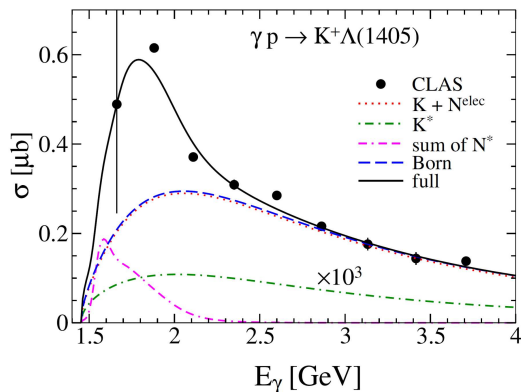


Fig. 3. Total cross-section for  $\gamma p \rightarrow K^+ \Lambda(1405)$  as a function of the beam energy,  $E_\gamma$ . The dot-double-dashed curve depicts, among other  $N^*$ 's, the contribution from the  $N^*(1895)$  exchange, which is found to be the dominant. The data are taken from [17].

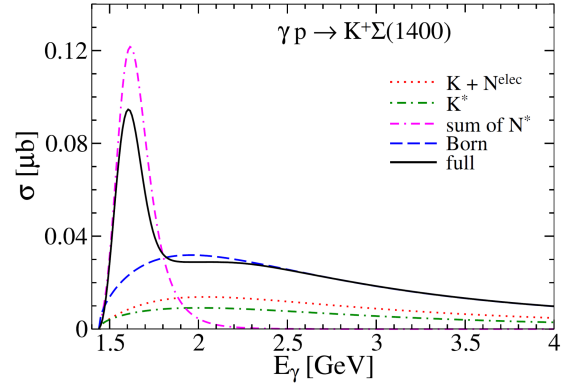


Fig. 4. Total cross-section for  $\gamma p \rightarrow K^+ \Sigma(1400)$  as a function of the beam energy,  $E_\gamma$ . Here the (magenta) dot-double-dashed curve depicts the contribution from the  $s$ -channel diagram with the  $N^*(1895)$  exchange.

to cross-sections larger than those obtained from the total amplitude, which indicates a negative interference occurs between different contributions. We hope that our findings motivate future experimental investigations of the photoproduction of  $\Sigma(1400)$ . It should be mentioned that results on different polarization observables are also shown and discussed in [35].

### 3. Conclusions

We can summarize the findings of our works presented at the conference by mentioning that the description of the properties of  $N^*(1895)$  necessarily requires important contributions from hadron dynamics. This nucleon resonance couples strongly to light hyperons ( $\Lambda(1405)$  and  $\Sigma(1400)$ ) and the related decay widths are comparable to the processes involving other meson-baryon channels. Here  $\Sigma(1400)$  is a  $1/2^-$  resonance, whose existence is still not certain and requires further experimental investigations. Our findings show that  $N^*(1895)$  exchange gives important contributions to the cross-sections of photoproduction of  $\Lambda(1405)$  as well as  $\Sigma(1400)$ . There exist data on the photoproduction of  $\Lambda(1405)$ , and our results are in good agreement with this data. Our findings on the cross-sections for  $\Sigma(1400)$  are predictions and should serve as a motivation for experimental investigations of the process, which should be useful in establishing the existence of the state with better certainty.

### Acknowledgments

K.P.K and A.M.T gratefully acknowledge the support from the Fundação de Amparo à Pesquisa do Estado de São Paulo (FAPESP), processos n° 2019/17149-3 and 2019/16924-3, by the Conselho Nacional de Desenvolvimento Científico e Tecnológico (CNPq), grants n° 305526/2019-7 and

303945/2019-2. A.M.T also thanks the partial support from mobilidade Santander (edital PRPG no 11/2019). H.N. is supported in part by Grants-in-Aid for Scientific Research (JP17K05443 (C)). AH is supported in part by Grants-in-Aid for Scientific Research (JP17K05441 (C)) and for Scientific Research on Innovative Areas (No. 18H05407). S.H.K. and S.i.N thank National Research Foundation of Korea funded by the Ministry of Education, Science and Technology (MSIT) (NRF-2019R1C1C1005790 (S.H.K.), 2018R1A5A1025563, and 2019R1A2C1005697).

### References

- [1] A. Scordo, M. Bazzi, G. Bellotti et al., *AIP Conf. Proc.* **1735**, 080015 (2016).
- [2] M. Skurzok, M. Cargnelli, C. Curceanu et al., *Acta Phys. Pol. B* **49**, 705 (2018).
- [3] E. Friedman, A. Gal, *EPJ Web Conf.* **181**, 01008 (2018).
- [4] D. Jido, J.A. Oller, E. Oset, A. Ramos, U.G. Meißner, *Nucl. Phys. A* **725**, 181 (2003).
- [5] T. Hyodo, D. Jido, *Prog. Part. Nucl. Phys.* **67**, 55 (2012).
- [6] C. Garcia-Recio, J. Nieves, E. Ruiz Arriola, M.J. Vicente Vacas, *Phys. Rev. D* **67**, 076009 (2003).
- [7] R.H. Dalitz, T.C. Wong, G. Rajasekaran, *Phys. Rev.* **153**, 1617 (1967).
- [8] V.K. Magas, E. Oset, A. Ramos, *Phys. Rev. Lett.* **95**, 052301 (2005).
- [9] M. Mai, U.G. Meißner, *Nucl. Phys. A* **900**, 51 (2013).
- [10] N. Kaiser, P.B. Siegel, W. Weise, *Nucl. Phys. A* **594**, 325 (1995).
- [11] E. Oset, A. Ramos, *Nucl. Phys. A* **635**, 99 (1998).
- [12] J.A. Oller, U.G. Meißner, *Phys. Lett. B* **500** (2001) 263.
- [13] A. Mueller-Groeling, K. Holinde, J. Speth, *Nucl. Phys. A* **513**, 557 (1990).
- [14] M. Mai, *Eur. Phys. J. Special Topics* **230**, 1593 (2021).
- [15] K. Moriya, R.A. Schumacher, K.P. Adhikari et al. (CLAS Collaboration), *Phys. Rev. C* **87**, 035206 (2013).
- [16] H.Y. Lu, R.A. Schumacher, K.P. Adhikari et al. (CLAS Collaboration), *Phys. Rev. C* **88**, 045202 (2013).
- [17] K. Moriya, R.A. Schumacher, K.P. Adhikari et al. (CLAS Collaboration), *Phys. Rev. C* **88**, 045201 (2013).
- [18] J.M.M. Hall, W. Kamleh, D.B. Leinweber, B.J. Menadue, B.J. Owen, A.W. Thomas, R.D. Young, *Phys. Rev. Lett.* **114**, 132002 (2015).
- [19] B.J. Menadue, W. Kamleh, D.B. Leinweber, M.S. Mahbub, *Phys. Rev. Lett.* **108**, 112001 (2012).
- [20] N. Ishii, T. Doi, M. Oka, H. Suganuma, *Prog. Theor. Phys. Suppl.* **168**, 598 (2007).
- [21] T.T. Takahashi, M. Oka, *Prog. Theor. Phys. Suppl.* **186**, 172 (2010).
- [22] J.M.M. Hall, W. Kamleh, D.B. Leinweber, B.J. Menadue, B.J. Owen, A.W. Thomas, *Phys. Rev. D* **95**, 054510 (2017).
- [23] P. Gubler, T.T. Takahashi, M. Oka, *Phys. Rev. D* **94**, 114518 (2016).
- [24] R.A. Briceno, J.J. Dudek, R.D. Young, *Rev. Mod. Phys.* **90**, 025001 (2018).
- [25] S.D. Bass, P. Moskal, *Rev. Mod. Phys.* **91**, 015003 (2019).
- [26] N.G. Kelkar, K.P. Khemchandani, N.J. Upadhyay, B.K. Jain, *Rep. Prog. Phys.* **76**, 066301 (2013).
- [27] Zhi-Hui Guo, J.A. Oller, *Phys. Rev. C* **87**, 035202 (2013).
- [28] J.J. Wu, S. Dulat, B.S. Zou, *Phys. Rev. D* **80**, 017503 (2009).
- [29] J.J. Wu, S. Dulat, B.S. Zou, *Phys. Rev. C* **81**, 045210 (2010).
- [30] P. Gao, J.J. Wu, B.S. Zou, *Phys. Rev. C* **81**, 055203 (2010).
- [31] J.J. Xie, J.J. Wu, B.S. Zou, *Phys. Rev. C* **90**, 055204 (2014).
- [32] J.J. Xie, L.S. Geng, *Phys. Rev. D* **95**, 074024 (2017).
- [33] K.P. Khemchandani, A. Martínez Torres, H. Nagahiro, A. Hosaka, *Phys. Rev. D* **85**, 114020 (2012).
- [34] K.P. Khemchandani, A. Martínez Torres, J.A. Oller, *Phys. Rev. C* **100**, 015208 (2019).
- [35] S.H. Kim, K.P. Khemchandani, A. Martínez Torres, S.I. Nam, A. Hosaka, *Phys. Rev. D* **103**, 114017 (2021).
- [36] G. Scheluchin, S. Alef, P. Bauer et al., *EPJ Web Conf.* **241**, 01014 (2020).
- [37] K.P. Khemchandani, A. Martínez Torres, H. Nagahiro, A. Hosaka, *Phys. Rev. D* **88**, 114016 (2013).
- [38] K.P. Khemchandani, A. Martínez Torres, H. Nagahiro, A. Hosaka, *Phys. Rev. D* **103**, 016015 (2021).
- [39] K.P. Khemchandani, H. Kaneko, H. Nagahiro, A. Hosaka, *Phys. Rev. D* **83**, 114041 (2011).
- [40] U.G. Meißner, *Rep. Prog. Phys.* **56**, 903 (1993).
- [41] G. Ecker, *Prog. Part. Nucl. Phys.* **35**, 1 (1995).
- [42] A. Pich, *Rep. Prog. Phys.* **58**, 563 (1995).

- [43] J.A. Oller, M. Verbeni, J. Prades, *J. High Energy Phys.* **2006**, 079 (2006).
- [44] K.P. Khemchandani, A. Martinez Torres, H. Kaneko, H. Nagahiro, A. Hosaka, *Phys. Rev. D* **84** 094018 (2011).
- [45] M. Bazzi, G. Beer, L. Bombelli et al. (SIDDHARTA Collaboration), *Phys. Lett. B* **704**, 113 (2011).
- [46] A. Baldini, V. Flaminio, W. I. G. Moorhead, D. R. O. Morrison, in: *Total Cross-Sections for Reactions of High Energy Physics* Vol. 12a, Ed. H. Schopper, Springer, Berlin 1988.
- [47] R.A. Arndt, I.I. Strakovsky, R.L. Workman, M.M. Pavan, *Phys. Rev. C* **52**, 2120 (1995).
- [48] T. Mart, C. Bennhold, *Phys. Rev. C* **61**, 012201 (2000).
- [49] A.V. Anisovich, R. Beck, E. Klempt, V.A. Nikonov, A.V. Sarantsev, U. Thoma, *Eur. Phys. J. A* **48**, 15 (2012).
- [50] T. Mart, *Phys. Rev. D* **100**, 056008 (2019).
- [51] T. Mart, M.J. Kholili, *Phys. Rev. C* **86**, 022201 (2012).
- [52] A. Martinez Torres, K.P. Khemchandani, U.G. Meissner, E. Oset, *Eur. Phys. J. A* **41**, 361 (2009).
- [53] N. Isgur, G. Karl, *Phys. Rev. D* **18**, 4187 (1978).
- [54] R. Bijker, F. Iachello, A. Leviatan, *Annals Phys.* **236**, 69 (1994).
- [55] A. Hosaka, H. Toki, M. Takayama, *Mod. Phys. Lett. A* **13**, 1699 (1998).
- [56] M. Takayama, H. Toki, A. Hosaka, *Prog. Theor. Phys.* **101**, 1271 (1999).
- [57] P.A. Zyla, R.M. Barnett, J. Beringer et al. (Particle Data Group), *Prog. Theor. Exp. Phys.* **2020**, 083C01 (2020).
- [58] L. Roca, J. Palomar, E. Oset, *Phys. Rev. D* **70**, 094006 (2004).
- [59] V.G.J. Stoks, T.A. Rijken, *Phys. Rev. C* **59**, 3009 (1999).
- [60] T.A. Rijken, V.G.J. Stoks, Y. Yamamoto, *Phys. Rev. C* **59**, 21 (1999).